European Cells and Materials Vol.53 2025 (pages 1–14) DOI: 10.22203/eCM.v053a01 ISSN 1473-2262

Original Article

MATRINE NANOPARTICLES IMPROVE FUNCTIONAL CONSTIPATION AND ASSOCIATED DEPRESSIVE BEHAVIORAL DISORDERS BY MODULATING THE GUT-BRAIN AXIS

J. Liu[1,2,§], S.K. Mu[3,§], J.X. Gao[4] and X.Y. Yan[1,*]

[1]Department of Geriatric Medicine, Affiliated Hospital of Shandong University of Traditional Chinese Medicine, 250011 Jinan, Shandong, China
[2]Postdoctoral Research Station, Shandong University of Traditional Chinese Medicine, 250011 Jinan, Shandong, China
[3]Department of Orthopedics, Hospital of Traditional Chinese Medicine of Liao Cheng City, 252000 Liaocheng, Shandong, China
[4]Surgery center, Affiliated Hospital of Shandong University of Traditional Chinese Medicine, 250011 Jinan, Shandong, China
[§]These authors contributed equally.

Abstract

Background: Functional constipation (FC) in the elderly is associated with depressive behavior. Matrine is a bioactive alkaloid with anti-inflammatory properties, promoting intestinal motility and gut barrier function. This study aimed to investigate how chitosan/matrine-poly(lactic-co-glycolic acid) nanoparticles (matrine NPs) alleviate depression in elderly mice with FC induced by loperamide (Lop). **Methods:** Matrine NPs were prepared, and their physical and chemical properties were determined by scanning electron microscopy, dynamic light scattering, and ultraviolet spectrophotometry. A Lop-induced FC model was established in C57BL/6J mice, and hematoxylin and eosin staining was used to assess inflammation and structural damage in colon tissue and hippocampus. The expression levels of occludin in colon tissue and ionized calcium binding adapter molecule 1 in the hippocampus were determined by immunohistochemistry. Enzyme-linked immunosorbent assay was employed to measure the levels of lipopolysaccharide, 5-hydroxytryptamine, and γ-aminobutyric acid in serum. The expression levels of genes related to gut barrier function and mucus secretion in the colon tissue, as well as genes related to inflammation and neuroimmune regulation in the hippocampus, were determined by quantitative reverse transcription polymerase chain reaction. The levels of short-chain fatty acid (SCFA) metabolites in mouse feces were measured using gas chromatography. The antidepressant effects of matrine NPs were evaluated through behavioral tests. **Results:** The release rate of matrine NPs reached 81.22 % in a simulated gastrointestinal environment. The drug loading (DL) and encapsulation efficiency (EE) of matrine NPs were 80.66 % $\pm$ 4.18 % and 69.37 % $\pm$ 2.86 %, respectively. Matrine NPs alleviated constipation symptoms, upregulated the expression of occludin in colon tissue, and effectively prevented gut barrier damage ($p < 0.001$). They also lessened anxiety and depression-like behaviors in FC mice by reducing synaptic degeneration and neuroinflammation ($p < 0.001$). Moreover, matrine NPs increased the levels of SCFAs in the feces ($p < 0.001$). **Conclusions:** The intake of matrine NPs alleviates depression caused by constipation in mice through the gut-brain axis.

Keywords: Matrine, gut-brain axis, functional constipation.

***Address for correspondence**: X.Y. Yan, Department of Geriatric Medicine, Affiliated Hospital of Shandong University of Traditional Chinese Medicine, 250011 Jinan, Shandong, China. Email: sharon.yan@163.com.

Introduction

Functional constipation (FC) is a common gastrointestinal condition characterized by infrequent bowel movements, difficulties in passing gas, and a sense of incomplete evacuation [1,2]. It significantly impacts the quality of life and is frequently associated with psychological symptoms such as anxiety and depression [3,4]. Despite its high prevalence, the underlying mechanisms of FC and its comorbidities remain poorly understood, and current therapeutic options are often inadequate, resulting in an ongoing need for effective treatments.

A recent investigation has demonstrated that the gut-brain axis plays a crucial role in the pathogenesis of functional gastrointestinal diseases [5]. The immune system, gut microbiota, enteric nervous system, and central nervous system are all involved in an intricate, two-way communication network known as the gut-brain axis [6]. Disruptions in this two-way communication network can lead to gastrointestinal symptoms and affect mental health, suggesting a potential link between FC and psychiatric disorders

[7,8]. In addition, stress-related behaviors have been reported in mice due to loperamide (Lop)-induced constipation [9]. Clinical data consistently link constipation with significant mental and psychological abnormalities [10].

Poly(lactic-co-glycolic acid) (PLGA) is extensively used as a biodegradable and biocompatible copolymer [11]. PLGA can undergo block polymerization with other copolymers to change the physical and chemical properties of a substance [12]. PLGA controls the biocompatibility, biodegradation, blood half-life, and targeting efficiency of particles [13]. Chitosan (CS) is a common biocompatible polymer that is widely used as a carrier for drugs, proteins, and other substances. In addition, it can be used as a nano-coating polymer [14]. CS is a natural biopolymer that is widely used in nanomaterials to increase the concentration of drugs and enhance the therapeutic effect. Studies have shown that the degradation of CS is mediated by the hydrolysis of the colonic biota cleavage of the glycosidic bond [15,16]. Moreover, nanoparticles (NPs) possess a positively charged surface that interacts electrostatically with the negative charged water-based mucin layer, resulting in a prolonged residence time within the mucus [17,18].

The traditional Chinese herb *Sophora flavescens* contains a bioactive alkaloid known as matrine. It has attracted attention for its diverse pharmacological characteristics, including anti-inflammatory, antiviral, and anticancer effects [19,20]. Previous research has indicated that matrine may modulate the immune response and improve intestinal barrier function, making it a promising candidate for treating inflammatory bowel diseases [21,22]. Matrine has been documented to regulate various neuronal pathways and exert neuroprotective effects [23]. A report from last year showed that matrine improves colitis in mice by reshaping gut microbiota [22]. However, its potential effects on FC and associated psychological symptoms have not been thoroughly investigated.

In this study, we aimed to establish a mouse model of FC and evaluate the therapeutic effects of CS/matrine-PLGA NPs (matrine NPs). We assessed the effects of matrine NPs on gut motility, colonic histopathology, and intestinal barrier function. Furthermore, we investigated its influence on mouse behaviors resembling anxiety and sadness, offering insights into the underlying mechanisms involving the gut-brain axis.

This research seeks to contribute to the development of novel therapeutic techniques for managing functional gastrointestinal diseases and improving patient outcomes by clarifying the effects of matrine NPs on FC and related psychological symptoms.

Materials and Methods

Preparation of Matrine NPs

For the preparation method, we referred to the study of Ünal *et al*. [24]. In this work, 2 % (w/v) PLGA and 20 mg of matrine were added to 10 mL of ethyl acetate. CS was dissolved in 0.2 % polyvinyl alcohol (PVA) to prepare a 25 mL solution. The 10 mL solution prepared in the first step was added to the 25 mL solution at the speed of 550 rpm to obtain the o/w emulsion. Ultrasound was performed four times at 25 °C, with each time lasting 1 min and comprising 10 s of exposure. The magnetic stirrer was used to stir the solution for 24 h, followed by centrifugation at 10,000 rpm for 45 min. The solution was rinsed four times in distilled water. Matrine NPs were added with 5 % (w/v) mannitol, lyophilized at −80 °C, and characterized. PLGA (HY-B2247, polylactic acid/polyglycolic acid = 50:50), CS (HY-B2144A), and PVA (HY-Y0850, Mw 146–186 kDa) were obtained from MedChemExpress (Monmouth County, NJ, USA).

Table 1. Primer sequences.

Primer name	Primer sequences (5′–3′)
Zo-1-F	ATGAGCTCCAGCAGTGAAGA
Zo-1-R	CTGGTAGGGAGTGAGTGGAG
Muc2-F	GGACCCACTTGCCACCTACT
Muc2-R	TTGCTGCTTGTGCTCTGGTT
Tff-3-F	CCTGCTGCTTCTGCTGCTC
Tff-3-R	CAGCCGGAAGTGATGTCATT
Iba-1-F	GCTTGAAGCTGACAGCACAG
Iba-1-R	TGTCCTCCTTGAGCACACAA
IL-1β-F	GCAACTGTTCCTGAACTCAACT
IL-1β-R	ATCTTTTGGGGTCCGTCAACT
TNF-α-F	AGGGTCTGGGCCATAGAACT
TNF-α-R	CCACCACGCTCTTCTGTCTAC
Trl4-F	CAGAGTTTCCTGCAATGGATCA
Trl4-R	TGTTCTCACACTGGCATCATC
Cox-2-F	GGGAGTCTGGAACATTGTGAA
Cox-2-R	CTCGGACACGTGTTGATGT
Nlrp3-F	TGGACCTTGGAGACACAGAT
Nlrp3-R	TGTGTGTGAAGATGCTGAGT
GAPDH-F	AGGTCGGTGTGAACGGATTTG
GAPDH-R	TGTAGACCATGTAGTTGAGGTCA

Zo-1, zonula occludens-1; Iba-1, ionized calcium binding adapter molecule 1; Muc2, mucin 2; Tff-3, trefoil factor 3; IL, interleukin; TNF, tumor necrosis factor; Trl4, toll-like receptor 4; Cox-2, cyclooxygenase-2; Nlrp3, NOD-like receptor thermal protein domain-associated protein 3; GAPDH, glyceraldehyde-3-phosphate dehydrogenase.

Table 2. Physicochemical property parameters of matrine NPs.

Nano-particles	EE (%)	DL (%)
Matrine NPs	69.37 % ± 2.86 %	80.66 % ± 4.18 %

EE, encapsulation efficiency; DL, drug loading; NPs, nanoparticles.

Scanning Electron Microscopy (SEM)

The surface morphology of matrine NPs was observed by SEM (Sigma 300, Zeiss, Oberkochen, Baden-

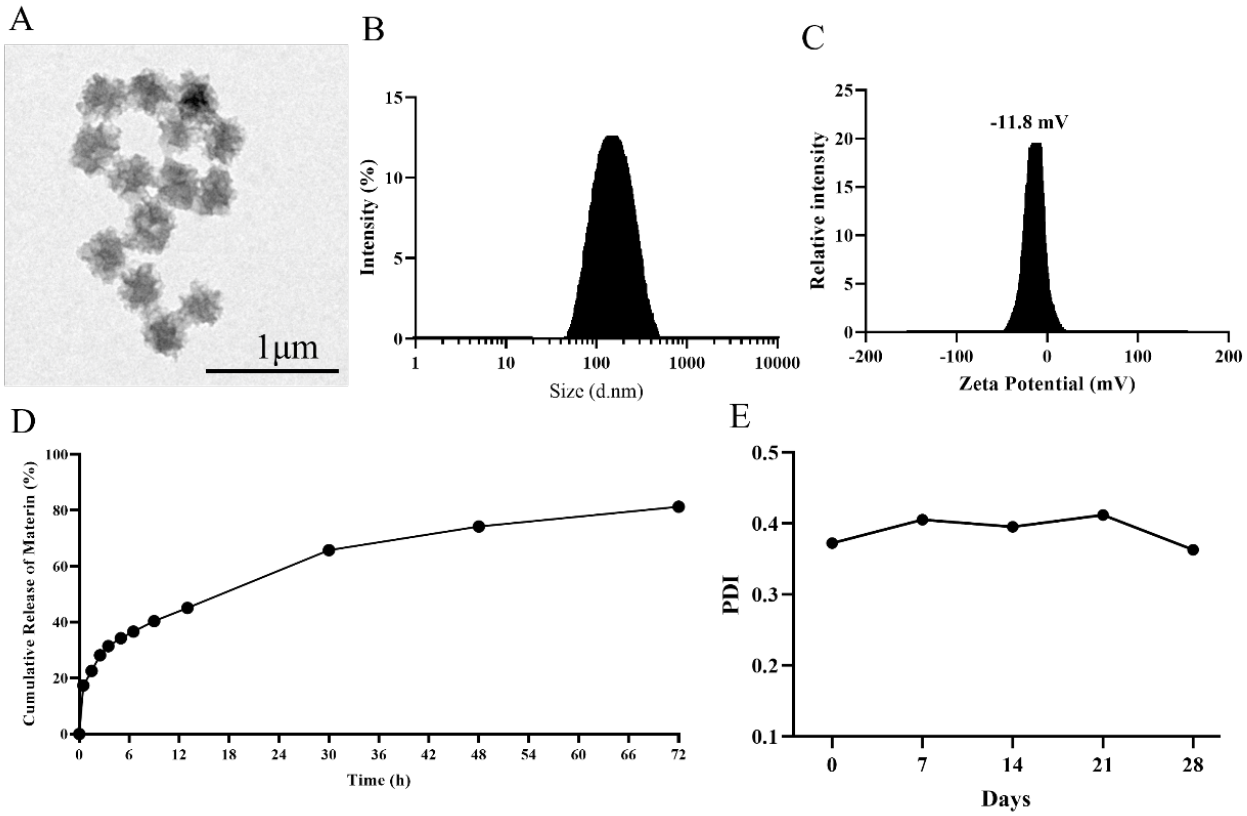

Fig. 1. Characterization of matrine NPs. (**A**) SEM image of matrine NPs. Scale bar: 1 μm. (**B**) Matrine NP size distribution. (**C**) Zeta potential analysis. (**D**) Release of matrine NPs *in vitro*. (**E**) PDI of matrine NPs. NPs, nanoparticles; SEM, scanning electron microscopy; PDI, polydispersity index. The images were plotted using GraphPad Prism 9.0 software.

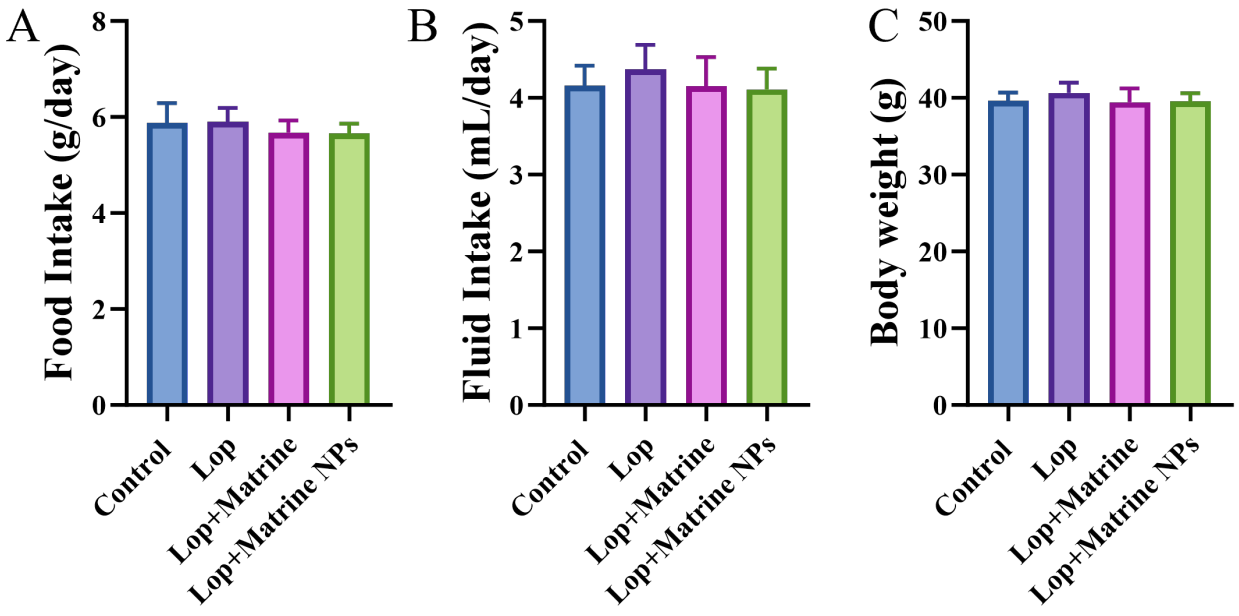

Fig. 2. Effects of matrine NPs on the physiological characteristics of FC mice. (**A**) Food intake. (**B**) Fluid intake of the mice. (**C**) Body weight of the mice (N = 6). FC, functional constipation; Lop, loperamide. The images were plotted using GraphPad Prism 9.0 software.

Württemberg, Germany). Matrine NPs were coated with a 100 A-thick coating of gold and palladium, inserted into a metal post, and dried for 24 h for SEM analysis. Morphology images were generated by introducing high-beam electrons and an accelerating voltage of 5/15 kV.

Characterization of Matrine NPs

The mean particle size, zeta potential, and polydispersity index (PDI) of matrine NPs were analyzed by dynamic light scattering (DLS; zs90, Malvern Instrument, Great Malvern, UK). The instrument setting parameters were as follows: particle size measurement of 173°; zeta potential measurement of 12.8°; and temperature of 25 °C.

Determination of Drug Loading (DL) Capacity

About 1 mL of methanol was added into the freeze-dried matrine NPs, and vortex ultrasound was performed for 1 min each. The sample was centrifuged at 6000 rpm for 10 min to extract the supernatant. Subsequently, 1 mL of ethanol was added to the precipitate, and the above steps were repeated to extract the drug completely. Finally, all the supernatants were mixed and measured at a wavelength of 230 nm via ultraviolet spectrophotometry (UV-1800, Nanjing Kojtech Analytical Instrument Co., Ltd., Nanjing, China). Encapsulation efficiency (EE) was calculated using the formula: EE = (Total amount of drug – Amount of free drug)/Total amount of drug × 100 %. Additionally, DL was determined by the following formula: DL = (Drug mass/Total carrier mass) × 100 %.

Drug Release Analysis

To simulate the environment in the gut, we used three different pH values for *in vitro* release studies. We used pH 1.2 for 2 h to simulate gastric fluid conditions, pH 6.8 for 3 h to simulate intestinal fluid, and pH 7.4 for 67 h to simulate colonic fluid.

Animal Experiment

Twenty-four male C57BL/6J mice aged 16 months were purchased from Shanghai Model Organisms (Shanghai, China). The mice were subjected to a light/dark period for 12 h, with humidity set to 50 %–60 % and a temperature of 23 °C ± 2 °C. The mice were randomly divided into four groups via a random number table: control, Lop, Lop + matrine, and Lop + matrine NP groups. Control group: Mice were provided with distilled water and a standard diet for 14 days. Lop group: Mice were provided with distilled water containing Lop (20 mg/kg) and a standard diet for 14 days to establish the FC model. Lop + matrine group: Mice were provided with distilled water containing Lop (20 mg/kg) and a standard diet containing matrine (40 mg/kg) for 14 days. Lop + matrine NP group: Mice were provided with distilled water containing Lop (20 mg/kg) and a standard diet containing matrine NPs (40 mg/kg) for 14 days. Once the FC mouse model was established, water and food intake were recorded every 3 days. Other behavioral tests were carried out, such as the raised plus maze, marble burying, tail suspension, and open field tests. At the end of the experiment, the mice were euthanized by inhaling excess isoflurane (R510-22, RWD, Shenzhen, China), followed by cervical dislocation. The animal protocol was designed to minimize pain or discomfort to the animals.

Behavioral Experiments

Open Field Test. Each group of mice was placed in a 40 cm × 40 cm darkly lit activity monitoring chamber for 5 min. The total distance traveled by the mice and the distance from the center area were promptly recorded.

Tail Suspension Test. We affixed a tail suspension apparatus to a stable surface. We then gently held the mouse and attached the end of its tail to the hook of the suspension apparatus with adhesive tape, ensuring the mouse was suspended and could not touch any surface. The suspension height should be consistent for each mouse. After starting the timer, we observe the mouse's behavior for 6 min. The duration of the mouse's struggling time (active period) and immobility time (inactive period) during the test were recorded.

Marble Burying Test. In this test, we evenly spread clean bedding material on the bottom of the mouse cage to a depth of about 5 cm. Subsequently, we arranged 20 glass marbles uniformly on the bedding surface in a 4 × 5 grid, maintaining a distance of 2 cm between each marble. We introduced the mouse into the designated cage and allowed it to explore freely for 30 min. The number of marbles that were completely or partially buried during the 30-min period was recorded.

Elevated Plus Maze Test. Before the experiment, we checked the stability and cleanliness of the elevated plus maze apparatus and sanitized it to prevent odors that might affect the behavior of the mice. The mouse was positioned at the central intersection of the elevated plus maze, facing an open arm. The timer was set to start, and we recorded the mouse's behavior for 5 min. The duration of the mice's stay in each arm and the number of times that the arms were opened and closed were noted.

Preparation of Serum Samples

The mice were anesthetized via intraperitoneal injection of sodium pentobarbital (40 mg/kg). The mice were secured in a specialized restraining device, and the periocular area was sanitized with 75 % alcohol. A microcapillary tube was gently inserted into the retro-orbital venous sinus area, rotating and applying slight pressure to facilitate blood flow into the tube. The serum was separated by centrifugation.

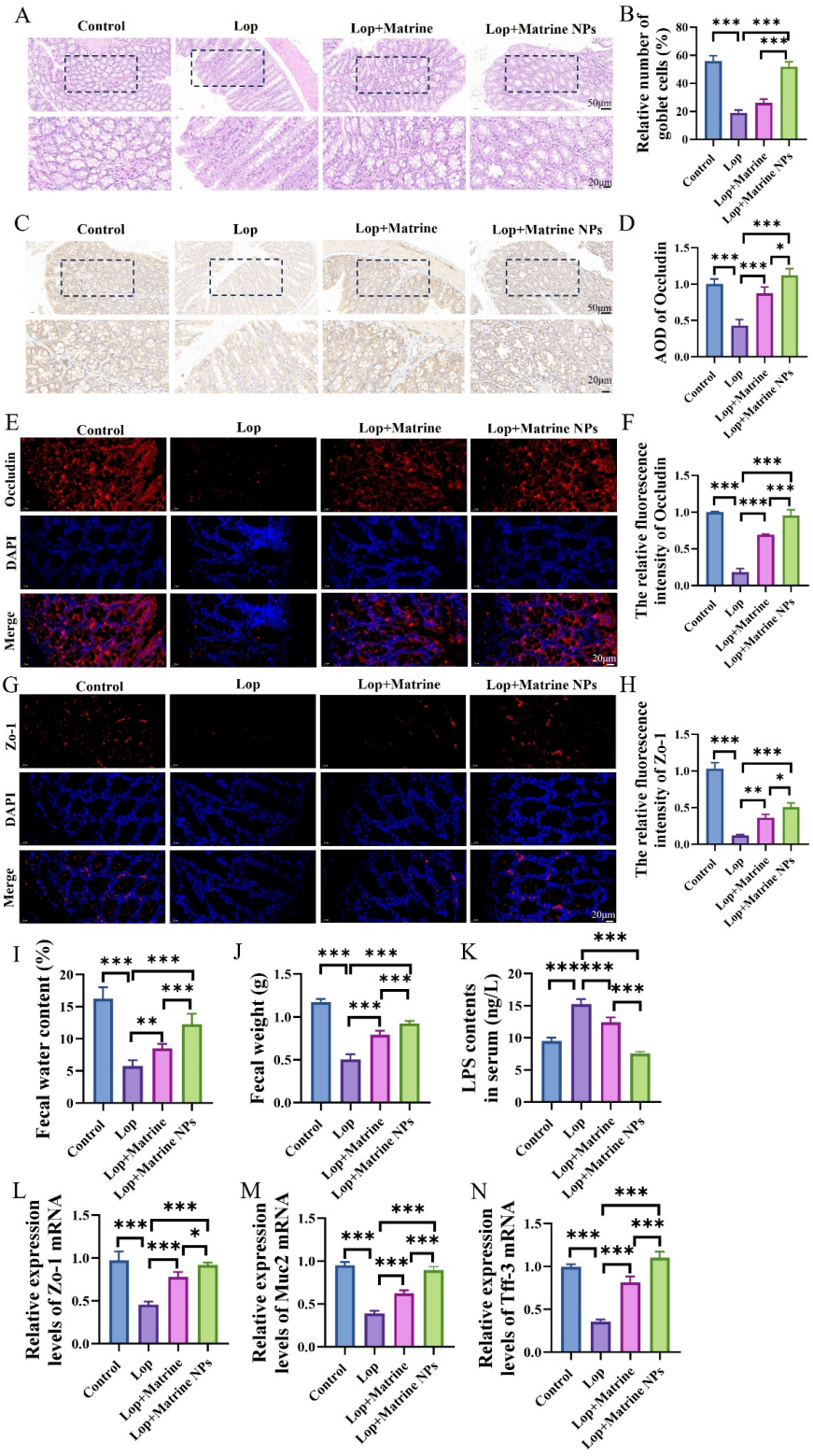

Fig. 3. Matrine NPs improve constipation and enhance intestinal barrier integrity in Lop-induced constipated mice. (**A,B**) Number of goblet cells and HE staining images in colon tissue (N = 3). Scale bar: 20 or 50 μm. (**C,D**) Immunohistochemical staining to detect occludin expression in mouse colon tissue (N = 3). Scale bar: 20 or 50 μm. (**E–H**) Immunofluorescence staining of occludin and Zo-1. Scale bar: 20 μm (N = 3). (**I**) Fecal water content. (**G**) Fecal weight. (**K**) Serum LPS levels. (**L–N**) mRNA expression levels of Zo-1, Muc2, and Tff-3 in colon tissue (N = 6). (*$p < 0.05$, **$p < 0.01$, ***$p < 0.001$). HE, hematoxylin and eosin; Zo-1, zonula occludens-1; LPS, lipopolysaccharide; Muc2, mucin 2; Tff-3, trefoil factor 3; mRNA, messenger ribonucleic acid; AOD, average optical density; DAPI, 4′,6-diamidino-2-phenylindole. The images were plotted using GraphPad Prism 9.0 software.

Hematoxylin and Eosin (HE) Staining

The colon tissue and hippocampus were fixed in 10 % neutral buffered formalin for 24–48 h. After fixation, the samples were dehydrated by sequentially immersing them in 70 %, 80 %, 90 %, 95 %, and 100 % ethanol for 15–30 min each. Subsequently, the samples were immersed twice in xylene for 10–20 min each time. The cleaned samples were embedded twice in molten paraffin at 60 °C for 30–60 min, followed by paraffin embedding. We cut the paraffin-embedded tissue into 4–5 μm-thick sections by using a microtome (Leica RM2235, Leica Biosystems, Nussloch, Germany). The sections were immersed on a 40 °C–45 °C water bath and transferred to glass slides. The slides were baked in 60 °C for 1–2 h to fix the sections. The slides were dewaxed by immersing them in xylene and rehydrated by sequentially immersing them in 100 %, 95 %, 90 %, 80 %, and 70 % ethanol, followed by distilled water. The slides were stained using an HE staining kit (G1120, Solarbio, Beijing, China), immersed in hematoxylin solution for 5–10 min, and rinsed with running water. The stains were differentiated in 1 % hydrochloric acid ethanol and turned blue with phosphate-buffered saline (PBS) or ammonia water. After the slides were stained in eosin solution for 1–2 min and rinsed with running water, they were dehydrated in ethanol series and cleared in xylene. Finally, mounting medium was applied to the slides, which were covered with coverslips to ensure the absence of air bubbles. The sections were observed with a microscope (DM6 B, Leica Microsystems, Wetzlar, Germany).

Immunohistochemistry

First, paraffin-embedded colon and hippocampal tissue sections were fixed onto slides and deparaffinized in xylene (two times for 10 min each). Second, the slides were rehydrated through ethanol solutions and rinsed with distilled water. Third, the slides were placed in a microwave-safe container with citrate buffer (pH 6.0) and heated in a microwave for 10–20 min to retrieve the antigen. The slides were cooled at room temperature for about 20 min and rinsed with PBS. Thereafter, the slides were immersed in 3 % hydrogen peroxide (H_2O_2, 88597, Merck Millipore, Billerica, MA, USA) for 10 min to block endogenous peroxidase activity, rinsed with PBS, and incubated with a blocking solution (5 % bovine serum albumin (BSA)) at room temperature for 30 min. We refrained from rinsing the slides after removing the excess blocking solution. Subsequently, the slides were incubated with the primary antibody and diluted in blocking solution (anti-occludin (ab216327, 1:1000) for colon tissue and anti-ionized calcium binding adapter molecule 1 (Iba-1) (ab178846, 1:1000) for hippocampal tissue) in a humidified chamber at 4 °C overnight. The primary antibodies were purchased from Abcam (Cambridge, MA, USA). The slides incubated with the secondary antibody were used for 30 min and then washed with PBS. They were incubated with the avidin-biotin complex reagent (PK-4001, Vector laboratories, Burlingame, CA, USA) for 30 min and rinsed with PBS. A diaminobenzidine (DAB) substrate kit (ab64238, Abcam, Cambridge, MA, USA) was used for color development according to the manufacturer's instructions, and the color was observed under a microscope. The reaction was stopped with distilled water when the color was suitable. Finally, the slides were dehydrated and cleared in xylene. Mounting medium was applied on the slides and covered with coverslips, ensuring no air bubbles. The sections were observed by using a microscope (DM6 B, Leica Microsystems, Wetzlar, Germany).

Immunofluorescence Analysis

The tissue sections were dewaxed, hydrated, and incubated with 3 % H_2O_2 at room temperature for 10 min. Cells were fixed with 4 % paraformaldehyde (P1110, Solarbio, Beijing, China). Thereafter, 0.3 % Triton-X (BL935B, Biosharp, Wuhan, China) was used for permeation at room temperature for 15 min, followed by the addition of 10 % normal goat serum (C0265, Beyotime Biotechnology, Shanghai, China) and incubation at room temperature for 2 h. The primary antibody (Abclonal, Wuhan, China) was incubated at 4 °C overnight, and the second antibody (AS060, Abclonal, Wuhan, China) was incubated at room temperature for 1 h. Finally, the images were observed by using a fluorescence microscope.

The primary antibodies were zonula occludens-1 (Zo-1, A11417), occludin (A2601), glail fibrillary acidicprotein (GFAP, A19058), and Iba-1 (A19776), cytokeratin 18 (CK18, A27298), Villin (A23273).

ELISA

Lipopolysaccharide (LPS; A39552S), 5-hydroxytryptamine (5-HT; EEL006), and γ-aminobutyric acid (γ-GABA; EEL065) enzyme-linked immunosorbent assay (ELISA) kits were purchased from Thermo Fisher Scientific (Waltham, MA, USA). Serum samples were collected and diluted accordingly. Standards and diluted serum samples were added to the corresponding wells of a 96-well ELISA plate. The capture antibody was added according to the instructions. The plate was rinsed 3–5 times with wash buffer to remove unbound substances. The enzyme-labeled detection antibody was added and incubated further. The substrate solution, typically 3,3′,5,5′-tetramethylbenzidine (TMB), was introduced and incubated at the appropriate temperature and time until the color developed sufficiently. After the stop solution was incorporated, we measured the absorbance at a fixed wavelength by using a microplate reader (ELx808, Agilent, Santa Clara, CA, USA) according to the instructions.

Quantitative Reverse Transcription Polymerase Chain Reaction (qRT-PCR)

Total RNA was extracted from tissues using TRIzol reagent (15596026, Invitrogen, Carlsbad, CA, USA). DNase treatment was applied to remove genomic DNA contamination. The isolated RNA was reverse transcribed into complementary deoxyribonucleic acid (cDNA) by using a cDNA reverse transcription kit (K16325, MBI, San Jose, CA, USA). The synthesized cDNA templates were then subjected to qPCR (LightCycler 96, Roche, Basel, Switzerland), with quantification performed using the fluorescent dye SYBR Green (SY1020, Solarbio, Beijing, China). Data collection and analysis were carried out using qPCR instrument software (LightCycler 96 Software, Roche, Basel, Switzerland), and relative quantification was performed using the $2^{-\Delta\Delta Ct}$ method. The primer sequences used in this study are listed in Table 1.

Gas Chromatography

Fresh fecal samples from mice were obtained and weighed to 0.2 g. An internal standard and an appropriate amount of distilled water were added, and the mixture was vortexed and sonicated to ensure the sufficient extraction of short-chain fatty acids (SCFAs). The sample was centrifuged, and the supernatant was used for analysis. The sample was derivatized and analyzed by a gas chromatograph (Agilent 7890B, 19091F-433, Agilent Technologies, Santa Clara, CA, USA) equipped with a flame ionization detector. We selected an HP-FFAP column (Agilent Technologies, Santa Clara, CA, USA) with the following specifications: length of 30 m, internal diameter of 0.25 mm, and film thickness of 0.25 μm. The gas chromatography operating parameters were set as follows: column temperature program: initial temperature of 100 °C, hold for 2 min; ramp rate of 10 °C/min; final temperature of 200 °C, hold for 5 min. Inlet temperature: 250 °C; detector temperature: 250 °C; carrier gas: typically nitrogen; flow rate: 1–2 mL/min. Injection volume: 1–2 μL. Split ratio: 10:1. After injection, we recorded the chromatogram and used the internal standard method to quantify the concentration of each SCFA. The actual concentration of SCFAs in the sample was calculated using a calibration curve.

Cell Culture

Mouse intestinal epithelial cells (MODE-K, BFN608006456, BLUEFBIO, Shanghai, China) were cultured in RPMI 1640 medium (PM150110, Procell, Wuhan, China) containing 10 % fetal bovine serum, 100 U/mL penicillin and 100 mg/mL streptomycin at 37 °C in a 5 % CO_2. The cells were divided into the control group, the LPS group, the NPs group and the matrine NPs group. For LPS stimulation, MODE-K cells were incubated with 200 ng/mL LPS (ST1470, Beyotime Biotechnology, Shanghai, China) for 48 h [25]. For NPs group and the matrine NPs group, MODE-K cells were incubated with 50 μg/mL NPs or matrine NPs [26]. MODE-K cells were mycoplasma-free.

5-Ethynyl-2′-Deoxyuridine (EdU) Assay

The cells in the logarithmic growth phase were resuspended to a concentration of 2×10^5 cells per milliliter. Then, 100 μL of the cell suspension was added to each well of a 96-well plate. Subsequently, 100 μL of the EdU solution (from kit C0085, Beiyue Biotechnology, Shanghai, China) was taken and added to each well separately. After that, 50 μL of 4% formaldehyde solution was added to each well to fix the cells for 30 minutes. The cells were then permeabilized using PBS containing 0.5% Triton X-100. The cell nuclei were stained with 4′,6-diamidino-2-phenylindole (DAPI) dye (C1006, Beyotime Biotechnology, Shanghai, China) and incubated in the dark for 5 min. The images were observed using a fluorescence microscope (CX41-32RFL, Olympus Corporation, Tokyo, Japan).

Clone Formation Assay

Cells in the logarithmic growth phase were taken and digested with trypsin (C0201, Beyotime Biotechnology, Shanghai, China). The cells were inoculated in 6-well plates, with 1000 cells in each well. 1 mL of 4 % paraformaldehyde was added to each well to fix the cells for 30 min, and then 1 mL of crystal violet (C0121, Beyotime Biotechnology, Shanghai, China) was added for staining for 10 min. Finally, the cells were observed through a microscope (BX46, Olympus Corporation, Tokyo, Japan).

Statistical Analysis

Using Tukey's post hoc test and one-way analysis of variance (ANOVA) in GraphPad Prism software (version 9.0, GraphPad Software, Inc., San Diego, CA, USA), comparisons across different groups were analyzed. Tukey's multiple correction method was used to adjust the *p*-value to control the false positive rate. $p < 0.05$ was considered statistically significant.

Results

Characterization of Matrine NPs and DLS Analysis

As shown in Fig. 1**A**, the surface of matrine NPs was smooth and spherical. As shown in Fig. 1**B**, the particle size of matrine NPs was 145.9 nm. Fig. 1**C** shows that the zeta potential of matrine NPs was −11.8 mV, whereas Fig. 1**D** shows the release curve of matrine NPs. Within 0–2 h, the maximum amount of matrine (about 26.58 %) was released. Within 2–6 h, the amount released decreased compared with that in the previous 2 h. When matrine NPs reached the simulated fluid environment of the colon, they could still maintain a release rate of 81.22 %. The stability of matrine NPs was determined by measuring size, PDI, and zeta potential over a 28-day period (Fig. 1**E**), and the results revealed that matrine NPs exhibited good stability within 28 days. Subsequently, the release curve of matrine NPs

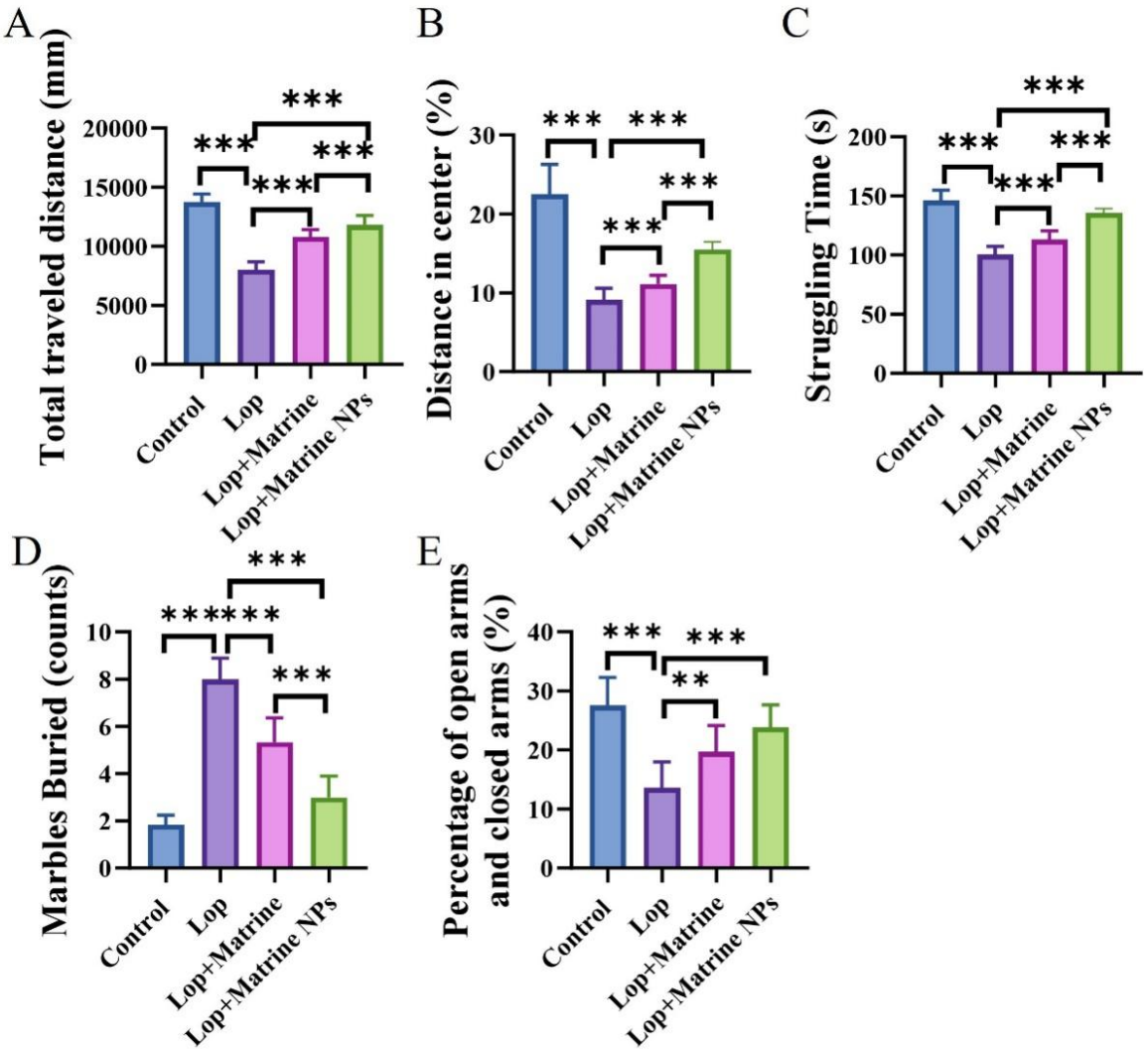

Fig. 4. Matrine NPs reverse depressive-like behavior in Lop-induced FC mice. (**A,B**) Total travel distance (**A**) and center distance (**B**) in the open field test. (**C**) Struggling time in the tail suspension test. (**D**) Number of buried marbles. (**E**) Percentage of time spent in open arms versus closed arms in the elevated plus maze (N = 6). (**$p < 0.01$, ***$p < 0.001$). The images were plotted using GraphPad Prism 9.0 software.

gradually flattened out until the end of the experiment. The DL and EE of the matrine NPs are shown in Table 2. The results showed that the DL and EE of matrine NPs were 80.66 % ± 4.18 % and 69.37 % ± 2.86 %, respectively.

Effects of Matrine NPs on the Physiological Characteristics of FC Mice

First, we identified MODE-K cells through cytomorphology and immunofluorescence staining of CK18 and Villin. The results indicated that MODE-K cells were polygonal or oval in shape, arranged in a typical "paving stone" pattern, and had strong positive signals of CK18 and Villin (**Supplementary Fig. 1**). Then, we explored the influence of NPs through cell counting kit-8 (CCK-8), EdU proliferation and clone formation (**Supplementary Fig. 2**). The experimental results show that there is no significant difference in the results between the NPs group and the LPS group. As shown in Fig. 2**A–C**, we found no significant differences in food intake, body weight, and fluid intake among the four groups of mice.

Matrine NPs Improve Lop-Induced Constipation in FC Mice and Enhance Gut Barrier Integrity

The results of Fig. 3**A,B** show that the Lop group exhibited disorganized cell arrangement, cytoplasmic vacuolation, and a significant reduction in the number of goblet cells ($p < 0.001$). However, matrine NP treatment significantly alleviated these symptoms and markedly increased the number of goblet cells ($p < 0.001$). The immunohistochemical staining results of the colon (Fig. 3**C,D**) revealed that occludin expression was significantly reduced after Lop treatment ($p < 0.001$). Nevertheless, matrine and

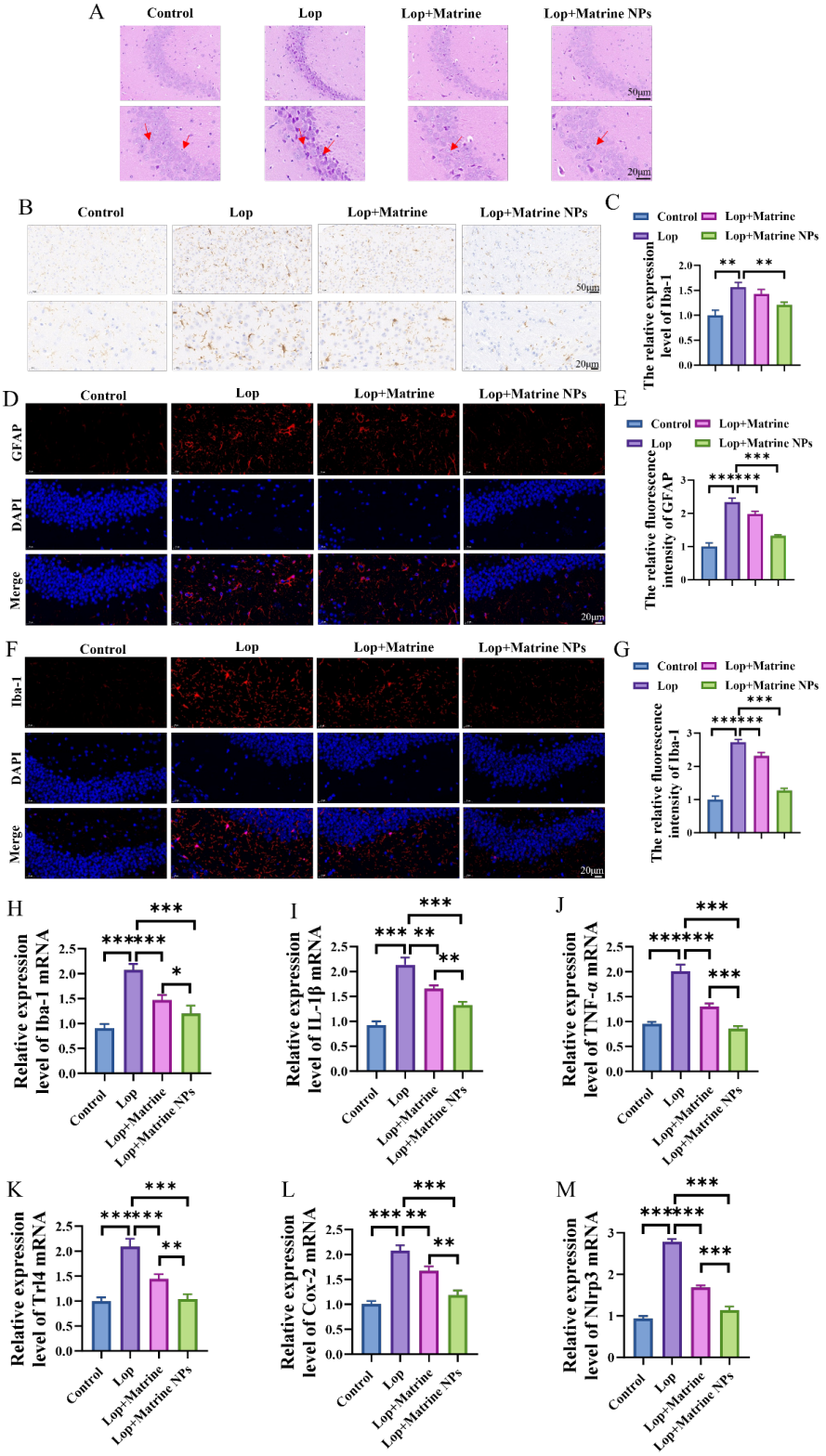

Fig. 5. Matrine NPs alleviate brain inflammation in Lop-induced FC mice. (**A**) HE staining of mouse hippocampal tissue (N = 3). Scale bar: 20 or 50 μm. (**B,C**) IHC staining of Iba-1 in mouse hippocampal tissue (N = 3). Scale bar: 20 or 50 μm. (**D–G**) Immunofluorescence staining of GFAP and Iba-1. Scale bar: 20 μm (N = 3). (**H**) mRNA expression levels of Iba-1 in the cerebral cortex. (**I–M**) mRNA levels of IL-1β, TNF-α, Trl4, Cox-2, and Nlrp3 in hippocampal tissue (N = 6). (*$p < 0.05$, **$p < 0.01$, ***$p < 0.001$). Iba-1, ionized calcium binding adapter molecule 1; IL, interleukin; TNF, tumor necrosis factor; Trl4, toll-like receptor 4; Cox-2, cyclooxygenase-2; Nlrp3, NOD-like receptor thermal protein domain-associated protein 3; GFAP, glail fibrillary acidicprotein; IHC, immunohistochemistry. The images were plotted using GraphPad Prism 9.0 software.

matrine NP treatment significantly increased occludin expression ($p < 0.001$), with the matrine NP group exhibiting significantly higher expression levels than the matrine group ($p < 0.05$). As shown in Fig. 3**E–H**, the fluorescence intensity of occludin and Zo-1 in the matrine NP group was significantly enhanced, evidenced by immunofluorescence staining ($p < 0.001$). Fig. 3**I,J** shows that the fecal water content ($p < 0.001$) and fecal weight ($p < 0.01$) in the Lop-induced constipation group significantly decreased. However, matrine NP treatment partially increased the level of fecal water and fecal weight ($p < 0.001$). Additionally, the LPS levels in Lop-treated mice were elevated but returned to normal levels after matrine NP treatment ($p < 0.001$; Fig. 3**K**). The qRT-PCR results (Fig. 3**L–N**) showed that the messenger ribonucleic acid (mRNA) levels of Zo-1, mucin 2 (Muc2), and trefoil factor 3 (Tff-3) were downregulated in the Lop group ($p < 0.001$), whereas matrine NP treatment increased the mRNA expression levels of Zo-1, Muc2, and Tff-3 in the colon tissue ($p < 0.001$).

Matrine NPs Reverse Depressive-Like Behavior in Lop-Induced FC Mice

As shown in Fig. 4**A,B**, the Lop group exhibited a significantly reduced total travel distance and ratio of center distance ($p < 0.001$), whereas matrine NP treatment significantly increased the total travel distance and ratio of center distance in mice ($p < 0.001$). The results of Fig. 4**C–E** indicated that Lop group mice exhibited reduced struggling time, increased number of buried marbles, and decreased percentage of open arm exploration compared with mice from the other groups. These results demonstrated that Lop-induced FC could lead to anxiety-like behavior in mice ($p < 0.001$). Notably, matrine NP treatment alleviated the anxiety-like behavior in mice ($p < 0.001$).

Matrine NPs Alleviate Brain Inflammation in Lop-Induced FC Mice

The incidence rates of brain damage and nuclear pyknosis were greater in the Lop group than in the other groups, as shown in Fig. 5**A**. However, matrine NP treatment showed an improvement in these conditions. Fig. 5**B,C** shows that Iba-1 expression in the cerebral cortex significantly increased in the Lop group ($p < 0.01$). Notably, matrine NP treatment significantly inhibited Iba-1 mRNA expression in the mouse brain ($p < 0.01$). The results of immunofluorescence staining showed that the fluorescence intensity of GFAP and Iba-1 decreased significantly in the matrine NP group ($p < 0.001$; Fig. 5**D–G**). This result was also confirmed in Fig. 5**H**. Additionally, we investigated the mRNA expression of interleukin (IL)-1β, tumor necrosis factor-α (TNF-α), toll-like receptor 4 (Trl4), cyclooxygenase-2 (Cox-2), and NOD-like receptor thermal protein domain-associated protein 3 (Nlrp3) via qRT-PCR. The mRNA levels of these inflammatory factors were dramatically lowered by matrine NP treatment, whereas they were significantly raised by Lop treatment ($p < 0.001$; Fig. 5**I–M**).

Matrine NPs Improve the Metabolic Profile of Lop-Induced FC Mice

The results of Fig. 6**A–D** showed that SCFAs (including acetate, propionate, butyrate, and valerate) in the feces were significantly reduced in Lop-induced depressive mice ($p < 0.001$). Matrine NP treatment effectively increased their concentrations ($p < 0.001$). Furthermore, we observed a downward tendency in the Lop group for mood-related gut microbiota metabolites such as 5-HT and γ-GABA; however, this trend was considerably reversed by matrine NP therapy ($p < 0.001$; Fig. 6**E,F**).

Discussion

This study established an FC mouse model and systematically evaluated the effects of matrine NPs in improving constipation and its related depressive behaviors. Our findings indicated that matrine NPs not only significantly alleviated constipation symptoms but also exhibited a notable therapeutic effect on constipation-induced depressive and anxiety-like behaviors.

In this study, the drug release of matrine NPs *in vitro* was analyzed by DLS. We found that matrine was released in large quantities during the first 2 h, possibly due to its absorption by CS on the NP surface. In a low pH environment, the initial interaction between the media resulted in the release of the matrine attached to CS on the NP surface. In addition, the rapid solubility of matrine NPs may be due to the easy dissolution of CS in a low-pH environment [27]. Subsequently, the release rate of matrine slowed down, possibly due to the quenching effect caused by the film formed by the CS coating on the NP surface. Using different pH values to simulate the intestinal environment, matrine can be released stably and continuously after CS encapsulation.

In our study, the Lop group of mice displayed histological characteristics associated with patients with constipation, including cytoplasmic vacuolation, a marked decrease in the number of goblet cells, and a disorganized colonic tissue structure. These findings were consistent with previous studies, indicating that the Lop-induced constipation model could effectively mimic the pathological characteristics of human FC [28,29]. Matrine NP treatment significantly alleviated these histological changes, increased the number of goblet cells, and notably restored occludin expression, suggesting its potential role in maintaining intestinal mucosal barrier function.

Additionally, matrine NPs significantly reduced the levels of the inflammatory marker LPS in the colonic tissue of mice in the Lop group, indicating its potent anti-inflammatory effects. The qRT-PCR results demonstrated that matrine NP treatment significantly increased the mRNA expression levels of Zo-1, Muc2, and Tff-3, thereby further supporting their protective role in intestinal barrier

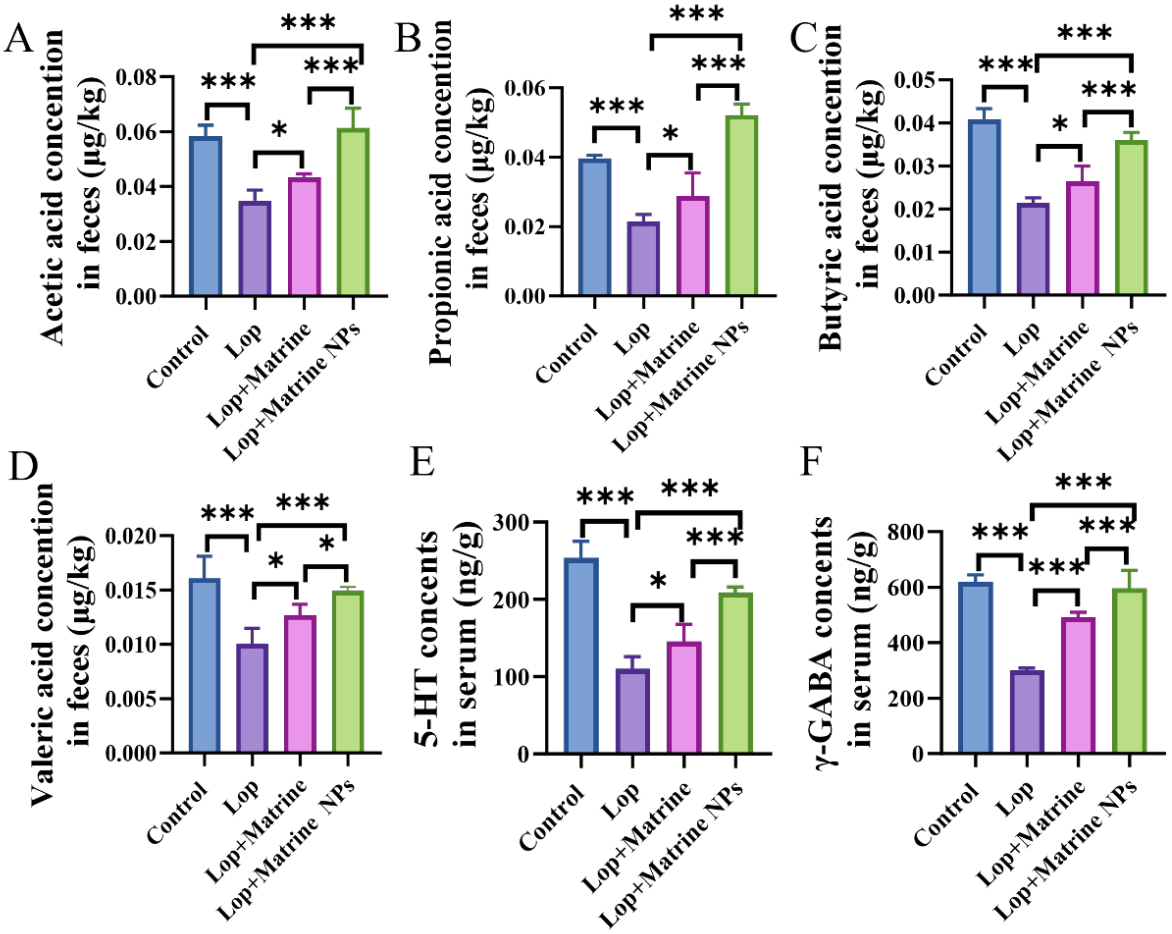

Fig. 6. Matrine NPs improve the content of gut metabolites in FC mice. (**A**) Acetate concentration in feces. (**B**) Propionate concentration in feces. (**C**) Butyrate concentration in feces. (**D**) Valerate concentration in feces. (**E**) 5-HT levels in serum. (**F**) γ-GABA levels in serum (N = 6). (*$p < 0.05$, ***$p < 0.001$). 5-HT, 5-hydroxytryptamine; γ-GABA, γ-aminobutyric acid. The images were plotted using GraphPad Prism 9.0 software.

function. These results were consistent with previous studies on matrine's anti-inflammatory effects, suggesting that matrine may alleviate constipation by modulating the intestinal inflammatory response [30,31].

Behavioral test results indicated that mice in the Lop group exhibited significant depressive and anxiety-like behaviors, including reduced total travel distance and center distance ratio, decreased struggling time, increased number of buried marbles, and diminished percentage of open arm exploration. These findings were consistent with existing research on the association between constipation and depression [32]. Notably, matrine NP treatment significantly improved these behavioral indicators, suggesting its therapeutic potential for constipation-related depression and anxiety.

In the hippocampus of mice in the Lop group, histopathological examination revealed a high frequency of nuclear pyknosis and neuronal injury in addition to markedly enhanced Iba-1 expression, suggesting a strong neuroinflammatory response. This result was similar to the characteristics of hippocampal neuroinflammation in depression model [33]. Matrine NP treatment significantly inhibited the expression of Iba-1 and reduced the mRNA levels of inflammatory factors IL-1β, TNF-α, Trl4, Cox-2, and Nlrp3 in the hippocampus, demonstrating its role in protecting hippocampal neurons and inhibiting neuroinflammation. These findings were consistent with previously reported effects of matrine in suppressing neuroinflammation [23,34].

Further research showed that Lop treatment significantly reduced the levels of SCFAs in the feces of mice, whereas matrine NP treatment effectively increased the concentrations of these SCFAs. SCFAs such as acetate, propionate, butyrate, and valerate play important roles in regulating gut health and brain function. Supplementation experiments with SCFAs indicated that the increase in SCFAs significantly improved Lop-induced behavioral abnormalities, further supporting the critical role of SCFAs in constipation and depression. In addition, this study indicated that the supplementation of dietary fiber and probiotics could

significantly improve FC, with an increase in SCFA levels, which was consistent with the results of a previous study [35]. This study can be used to supplement future work involving a probiotic or dietary fiber treatment group, and the obtained results can be compared with matrine NPs.

This study had some limitations. First, although mouse models play an important role in studying constipation and related depressive behaviors, they do not fully mimic the pathophysiological characteristics of humans. Second, the sample size of this study was small. Third, the study was conducted over a short time span, focusing mainly on acute and subacute stages, without evaluating the long-term effects and safety of matrine. Although the study revealed that matrine alleviated constipation and depressive behaviors by regulating gut barrier function, inhibiting inflammatory responses, and increasing SCFA concentrations, the specific molecular mechanisms require further exploration. Lastly, the current study data were entirely from animal experiments and have yet to be validated in clinical trials.

Future research should focus on assessing the long-term effects and safety of matrine, investigating its mechanisms within the gut-brain axis, and verifying its efficacy and safety in humans through multi-center, randomized controlled clinical trials. Further studies must analyze the effects of matrine on different subtypes of constipation and depression, explore personalized treatment strategies, and examine its combined effects with other treatments (such as probiotics, dietary fiber, and psychotherapy). By overcoming the current study's limitations and exploring new research directions, a comprehensive understanding of matrine's potential in treating constipation and depression can be achieved, providing a solid scientific basis for clinical applications. The sample size of this study must be further expanded and the SCFA treatment group added to demonstrate the link between SCFA and depressive behavior in mice. Finally, this study did not exclude the influence of PLGA and CS, so the PLGA/CS group should be designed in the subsequent experiment to discuss the potential confounding effect of NPs.

Conclusions

In summary, this study demonstrated the significant efficacy of matrine in improving Lop-induced FC mice and its related depressive and anxiety-like behaviors. The mechanisms of its action may include regulating gut barrier function, inhibiting intestinal and neuroinflammatory responses, and restoring SCFA levels. Our research provides strong evidence for matrine as a potential therapeutic drug for FC and related psychological disorders, but further clinical studies are needed to verify its effectiveness and safety.

List of Abbreviations

Lop, loperamide; SEM, scanning electron microscopy; DLS, dynamic light scattering; FC, functional constipation; HE, hematoxylin and eosin; Iba-1, ionized calcium binding adapter molecule 1; ELISA, enzyme-linked immunosorbent assay; LPS, lipopolysaccharide; 5-HT, 5-hydroxytryptamine; γ-GABA, γ-aminobutyric acid; qRT-PCR, quantitative reverse transcription polymerase chain reaction; SCFA, short-chain fatty acid; PLGA, poly(lactic-co-glycolic acid); CS, chitosan; EE, encapsulation efficiency; DL, drug loading; PBS, phosphate-buffered saline; Zo-1, zonula occludens-1; Muc2, mucin 2; Tff-3, trefoil factor 3; TNF, tumor necrosis factor; Trl4, toll-like receptor 4; Cox-2, cyclooxygenase-2; Nlrp3, NOD-like receptor thermal protein domain-associated protein 3; GAPDH, glyceraldehyde-3-phosphate dehydrogenase; NPs, nanoparticles; PVA, polyvinyl alcohol; PDI, polydispersity index; IL, interleukin; mRNA, messenger ribonucleic acid; DAPI, 4′,6-diamidino-2-phenylindole; GFAP, glail fibrillary acidicprotein; CK18, cytokeratin 18; cDNA, complementary deoxyribonucleic acid; EdU, 5-ethynyl-2′-deoxyuridine.

Availability of Data and Materials

The datasets used and analysed during the current study were available from the corresponding author on reasonable request.

Author Contributions

JL contributed to the design of this work. SKM contributed to the interpretation of data. JXG and XYY analyzed the data. SKM and XYY drafted the work. JXG and JL revised critically for important intellectual content. All authors read and approved the final manuscript. All authors agreed to be accountable for all aspects of the work in ensuring that questions related to the accuracy or integrity of any part of the work were appropriately investigated and resolved.

Ethics Approval and Consent to Participate

All animal procedures were performed in accordance with the Guidelines for the Care and Use of Laboratory Animals of Affiliated Hospital of Shandong University of Traditional Chinese Medicine. The study was approved by the Institutional Animal Care and Use Committee of Affiliated Hospital of Shandong University of Traditional Chinese Medicine (Approval No. (2024) Provincial Natural Basic Experiment Declaration (150)).

Acknowledgments

The brain (https://doi.org/10.5281/zenodo.3925903), gut (https://doi.org/10.5281/zenodo.3926408), and mouse (https://doi.org/10.5281/zenodo.3925901) images in the graphical abstract are respectively from Luigi Petrucco,

John Chilton, and Ethan Tyler (https://scidraw.io/).

Funding

Bureau-province co-construction project (GZY-KJS-SD-2023-044).

Conflict of Interest

The authors declare no conflict of interest.

Supplementary Material

Supplementary material associated with this article can be found, in the online version, at https://doi.org/10.22203/eCM.v053a01.

References

[1] Yurtdaş Depboylu G, Acar Tek N, Akbulut G, Günel Z, Kamanlı B. Functional Constipation in Elderly and Related Determinant Risk Factors: Malnutrition and Dietary Intake. Journal of the American Nutrition Association. 2023; 42: 541–547. https://doi.org/10.1080/27697061.2022.2096150.

[2] Chojnacki C, Mędrek-Socha M, Błońska A, Błasiak J, Popławski T, Chojnacki J, *et al*. A Low FODMAP Diet Supplemented with L-Tryptophan Reduces the Symptoms of Functional Constipation in Elderly Patients. Nutrients. 2024; 16: 1027. https://doi.org/10.3390/nu16071027.

[3] Yang C, Hu T, Xue X, Su X, Zhang X, Fan Y, *et al*. Multi-omics analysis of fecal microbiota transplantation's impact on functional constipation and comorbid depression and anxiety. BMC Microbiology. 2023; 23: 389. https://doi.org/10.1186/s12866-023-03123-1.

[4] Lv CL, Song GQ, Liu J, Wang W, Huang YZ, Wang B, *et al*. Colorectal motility patterns and psychiatric traits in functional constipation and constipation-predominant irritable bowel syndrome: A study from China. World Journal of Gastroenterology. 2023; 29: 5657–5667. https://doi.org/10.3748/wjg.v29.i41.5657.

[5] Frieling T, Gjini B, Melchior I, Euler P, Kreysel C, Kalde S, *et al*. Endoscopic laser endomicroscopy and "leaky gut" in patients with functional gastrointestinal symptoms and food intolerance. Zeitschrift für Gastroenterologie. 2023; 61: 1465–1471. https://doi.org/10.1055/a-1959-3200.

[6] Loh JS, Mak WQ, Tan LKS, Ng CX, Chan HH, Yeow SH, *et al*. Microbiota-gut-brain axis and its therapeutic applications in neurodegenerative diseases. Signal Transduction and Targeted Therapy. 2024; 9: 37. https://doi.org/10.1038/s41392-024-01743-1.

[7] Bonifacio C, Savini G, Reca C, Garoli F, Levi R, Vatteroni G, *et al*. The gut-brain axis: Correlation of choroid plexus volume and permeability with inflammatory biomarkers in Crohn's disease. Neurobiology of Disease. 2024; 192: 106416. https://doi.org/10.1016/j.nbd.2024.106416.

[8] Delprete C, Rimondini Giorgini R, Lucarini E, Bastiaanssen TFS, Scicchitano D, Interino N, *et al*. Disruption of the microbiota-gut-brain axis is a defining characteristic of the α-Gal A (-/0) mouse model of Fabry disease. Gut Microbes. 2023; 15: 2256045. https://doi.org/10.1080/19490976.2023.2256045.

[9] Li R, Xu S, Li B, Zhang B, Chen W, Dai D, *et al*. Gut indigenous *Ruminococcus gnavus* alleviates constipation and stress-related behaviors in mice with loperamide-induced constipation. Food & Function. 2023; 14: 5702–5715. https://doi.org/10.1039/d2fo03574j.

[10] Zheng S, Yao J, Chinese Geriatric Society, Editorial Board of Chinese Journal of Geriatrics. Expert consensus on the assessment and treatment of chronic constipation in the elderly. Aging Medicine. 2018; 1: 8–17. https://doi.org/10.1002/agm2.12013.

[11] Rocha CV, Gonçalves V, da Silva MC, Bañobre-López M, Gallo J. PLGA-Based Composites for Various Biomedical Applications. International Journal of Molecular Sciences. 2022; 23: 2034. https://doi.org/10.3390/ijms23042034.

[12] Sah E, Sah H. Recent Trends in Preparation of Poly(lactide-*co*-glycolide) Nanoparticles by Mixing Polymeric Organic Solution with Antisolvent. Journal of Nanomaterials. 2015; 2015: 794601. https://doi.org/10.1155/2015/794601.

[13] Rezvantalab S, Drude NI, Moraveji MK, Güvener N, Koons EK, Shi Y, *et al*. PLGA-Based Nanoparticles in Cancer Treatment. Frontiers in Pharmacology. 2018; 9: 1260. https://doi.org/10.3389/fphar.2018.01260.

[14] Chen MC, Mi FL, Liao ZX, Hsiao CW, Sonaje K, Chung MF, *et al*. Recent advances in chitosan-based nanoparticles for oral delivery of macromolecules. Advanced Drug Delivery Reviews. 2013; 65: 865–879. https://doi.org/10.1016/j.addr.2012.10.010.

[15] Tao Y, Zhao X, Liu X, Wang P, Huang Y, Bo R, *et al*. Oral delivery of chitosan-coated PLGA nanoemulsion loaded with artesunate alleviates ulcerative colitis in mice. Colloids and Surfaces. B, Biointerfaces. 2022; 219: 112824. https://doi.org/10.1016/j.colsurfb.2022.112824.

[16] Kosaraju SL. Colon targeted delivery systems: review of polysaccharides for encapsulation and delivery. Critical Reviews in Food Science and Nutrition. 2005; 45: 251–258. https://doi.org/10.1080/10408690490478091.

[17] Luo C, Sun J, Du Y, He Z. Emerging integrated nanohybrid drug delivery systems to facilitate the intravenous-to-oral switch in cancer chemotherapy. Journal of Controlled Release: Official Journal of the Controlled Release Society. 2014; 176: 94–103. https://doi.org/10.1016/j.jconrel.2013.12.030.

[18] Ensign LM, Cone R, Hanes J. Oral drug delivery with polymeric nanoparticles: the gastrointestinal mucus barriers. Advanced Drug Delivery Reviews. 2012; 64: 557–570. https://doi.org/10.1016/j.addr.2011.12.009.

[19] Sun XY, Jia LY, Rong Z, Zhou X, Cao LQ, Li AH, *et al*. Research Advances on Matrine. Frontiers in Chemistry. 2022; 10: 867318. https://doi.org/10.3389/fchem.2022.867318.

[20] Wang X, Wu FP, Huang YR, Li HD, Cao XY, You Y, *et al*. Matrine suppresses NLRP3 inflammasome activation via regulating PTPN2/JNK/SREBP2 pathway in sepsis. Phytomedicine: International Journal of Phytotherapy and Phytopharmacology. 2023; 109: 154574. https://doi.org/10.1016/j.phymed.2022.154574.

[21] Yu D, Su D, Liu Z. Matrine Protects Intestinal Barrier Function via MicroRNA-155 Through ROCK1-Signaling Pathway. The Turkish Journal of Gastroenterology: The Official Journal of Turkish Society of Gastroenterology. 2023; 34: 831–838. https://doi.org/10.5152/tjg.2023.21884.

[22] Mao N, Yu Y, He J, Yang Y, Liu Z, Lu Y, *et al*. Matrine Ameliorates DSS-Induced Colitis by Suppressing Inflammation, Modulating Oxidative Stress and Remodeling the Gut Microbiota. International Journal of Molecular Sciences. 2024; 25: 6613. https://doi.org/10.3390/ijms25126613.

[23] Chhabra S, Mehan S. Matrine exerts its neuroprotective effects by modulating multiple neuronal pathways. Metabolic Brain Disease. 2023; 38: 1471–1499. https://doi.org/10.1007/s11011-023-01214-6.

[24] Ünal S, Doğan O, Aktaş Y. Orally administered docetaxel-loaded chitosan-decorated cationic PLGA nanoparticles for intestinal tumors: formulation, comprehensive *in vitro* characterization, and release kinetics. Beilstein Journal of Nanotechnology. 2022; 13: 1393–1407. https://doi.org/10.3762/bjnano.13.115.

[25] Yang L, Wu G, Wu Q, Peng L, Yuan L. METTL3 overexpression aggravates LPS-induced cellular inflammation in mouse intestinal epithelial cells and DSS-induced IBD in mice. Cell Death Discovery. 2022; 8: 62. https://doi.org/10.1038/s41420-022-00849-1.

[26] Alshetaili AS. Gefitinib loaded PLGA and chitosan coated PLGA nanoparticles with magnified cytotoxicity against A549 lung cancer

cell lines. Saudi Journal of Biological Sciences. 2021; 28: 5065–5073. https://doi.org/10.1016/j.sjbs.2021.05.025.

[27] Aldawsari HM, Alhakamy NA, Padder R, Husain M, Md S. Preparation and Characterization of Chitosan Coated PLGA Nanoparticles of Resveratrol: Improved Stability, Antioxidant and Apoptotic Activities in H1299 Lung Cancer Cells. Coatings. 2020; 10: 439. https://doi.org/10.3390/coatings10050439.

[28] Luo M, Xie P, Deng X, Fan J, Xiong L. Rifaximin Ameliorates Loperamide-Induced Constipation in Rats through the Regulation of Gut Microbiota and Serum Metabolites. Nutrients. 2023; 15: 4502. https://doi.org/10.3390/nu15214502.

[29] Duan T, Wang X, Dong X, Wang C, Wang L, Yang X, *et al*. Broccoli-Derived Exosome-like Nanoparticles Alleviate Loperamide-Induced Constipation, in Correlation with Regulation on Gut Microbiota and Tryptophan Metabolism. Journal of Agricultural and Food Chemistry. 2023; 71: 16568–16580. https://doi.org/10.1021/acs.jafc.3c04150.

[30] Luo D, Zou JW, Wang JH, Tian H, Xie HY, Zhu TX, *et al.* Undescribed matrine-type alkaloids from Sophora alopecuroides with anti-inflammatory activity. Phytochemistry. 2024; 218: 113954. https://doi.org/10.1016/j.phytochem.2023.113954.

[31] Gao BB, Wang L, Li LZ, Fei ZQ, Wang YY, Zou XM, *et al*. Beneficial effects of oxymatrine from Sophora flavescens on alleviating Ulcerative colitis by improving inflammation and ferroptosis. Journal of Ethnopharmacology. 2024; 332: 118385. https://doi.org/10.1016/j.jep.2024.118385.

[32] Zou H, Gao H, Liu Y, Zhang Z, Zhao J, Wang W, *et al.* Dietary inulin alleviated constipation induced depression and anxiety-like behaviors: Involvement of gut microbiota and microbial metabolite short-chain fatty acid. International Journal of Biological Macromolecules. 2024; 259: 129420. https://doi.org/10.1016/j.ijbiomac.2024.129420.

[33] Zhao T, Piao LH, Li DP, Xu SH, Wang SY, Yuan HB, *et al*. BDNF gene hydroxymethylation in hippocampus related to neuroinflammation-induced depression-like behaviors in mice. Journal of Affective Disorders. 2023; 323: 723–730. https://doi.org/10.1016/j.jad.2022.12.035.

[34] Li J, Cheng XY, Yang H, Li L, Niu Y, Yu JQ, *et al*. Matrine ameliorates cognitive deficits via inhibition of microglia mediated neuroinflammation in an Alzheimer's disease mouse model. Die Pharmazie. 2020; 75: 344–347. https://doi.org/10.1691/ph.2020.0395.

[35] Lai H, Li Y, He Y, Chen F, Mi B, Li J, *et al*. Effects of dietary fibers or probiotics on functional constipation symptoms and roles of gut microbiota: a double-blinded randomized placebo trial. Gut Microbes. 2023; 15: 2197837. https://doi.org/10.1080/19490976.2023.2197837.

Editor's note: The Scientific Editor responsible for this paper was Kai Zheng.

Received: 23rd January 2025; **Accepted**: 24th June 2025; **Published**: 30th September 2025